

## Supplementary Information

### Nanofocusing beyond the near-field diffraction limit via plasmonic

#### Fano resonance

Maowen Song,<sup>a,b,c</sup> Changtao Wang,<sup>a</sup> Zeyu Zhao,<sup>a</sup> Mingbo Pu,<sup>a</sup> Ling Liu,<sup>a</sup> Wei Zhang,<sup>a,c</sup> Honglin Yu,<sup>b</sup> and Xiangang Luo<sup>\*a</sup>

<sup>a</sup>State Key Laboratory of Optical Technologies on Nano-Fabrication and Micro-Engineering, Institute of Optics and Electronics, Chinese Academy of Science, P.O. Box 350, Chengdu 610209, China.

<sup>b</sup>Key Laboratory of Optoelectronic Technology and System, Ministry of Education, Chongqing University, Chongqing 400044, China.

<sup>c</sup>University of Chinese Academy of sciences, Beijing 100049, China

\* Email address: [lxg@ioe.ac.cn](mailto:lxg@ioe.ac.cn)

#### 1. Plasmon hybridization occurred in the silver nanoring

Because of the finite thickness of the nanoring wall, the plasmon mode of the nanodisk and the nanohole interact with each other, splitting the plasmon resonances into two new modes: a symmetric bonding mode ( $|\omega-\rangle$ ) with lower energy and an asymmetric anti-bonding mode ( $|\omega+\rangle$ ) with higher energy.<sup>1,2</sup> The plasmon hybridization model has been shown in fig. S1.

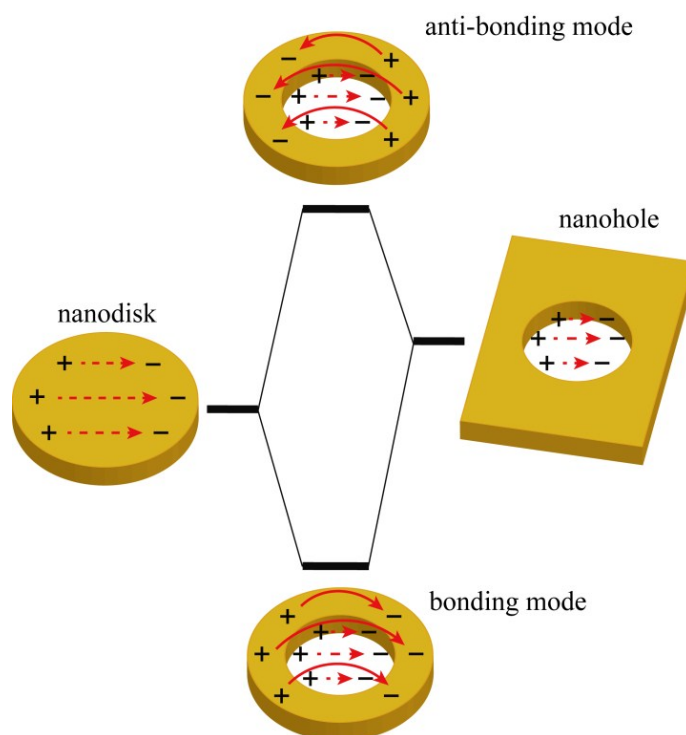


Fig. S1 Plasmon hybridization schemes of silver nanoring originated from the coupling between the nanodisk and nanohole's surface plasmons. The interference leads to the splitting with a symmetric bonding mode and an asymmetric anti-bonding mode.

Figure S2 describes the periodically arrayed silver nanorings with the optimized dimensions which will be discussed in the paper. Obviously, the spectrum possesses a strong resonance peak at 633 nm (indicated as  $P_1$ ). As depicted in the inset  $P_1$ , the electromagnetic fields profiles of a silver nanoring indicate that the resonance at 633 nm owes to the symmetric bonding mode.<sup>1</sup> The field distribution in the central nanohole shows opposite direction to that at the outer interface of the nanoring wall. The inset  $P_2$  and  $P_3$  intuitively reproduce the calculated spectrum with respect to the position and relative intensity of the resonance at  $P_2$  and  $P_3$  in the scattering parameters profile. For the other resonance at 410 nm ( $P_3$ ), it is clearly caused by the asymmetric anti-bonding mode. However, the resonance strength is too low to be seen clearly. From the view point of radiationless electromagnetic interference, the in-phase field distribution in different channels enhances radiation and therefore violates the REI rules to produce a radiationless static field pattern which is based on the out-of-phase interference of evanescent waves.

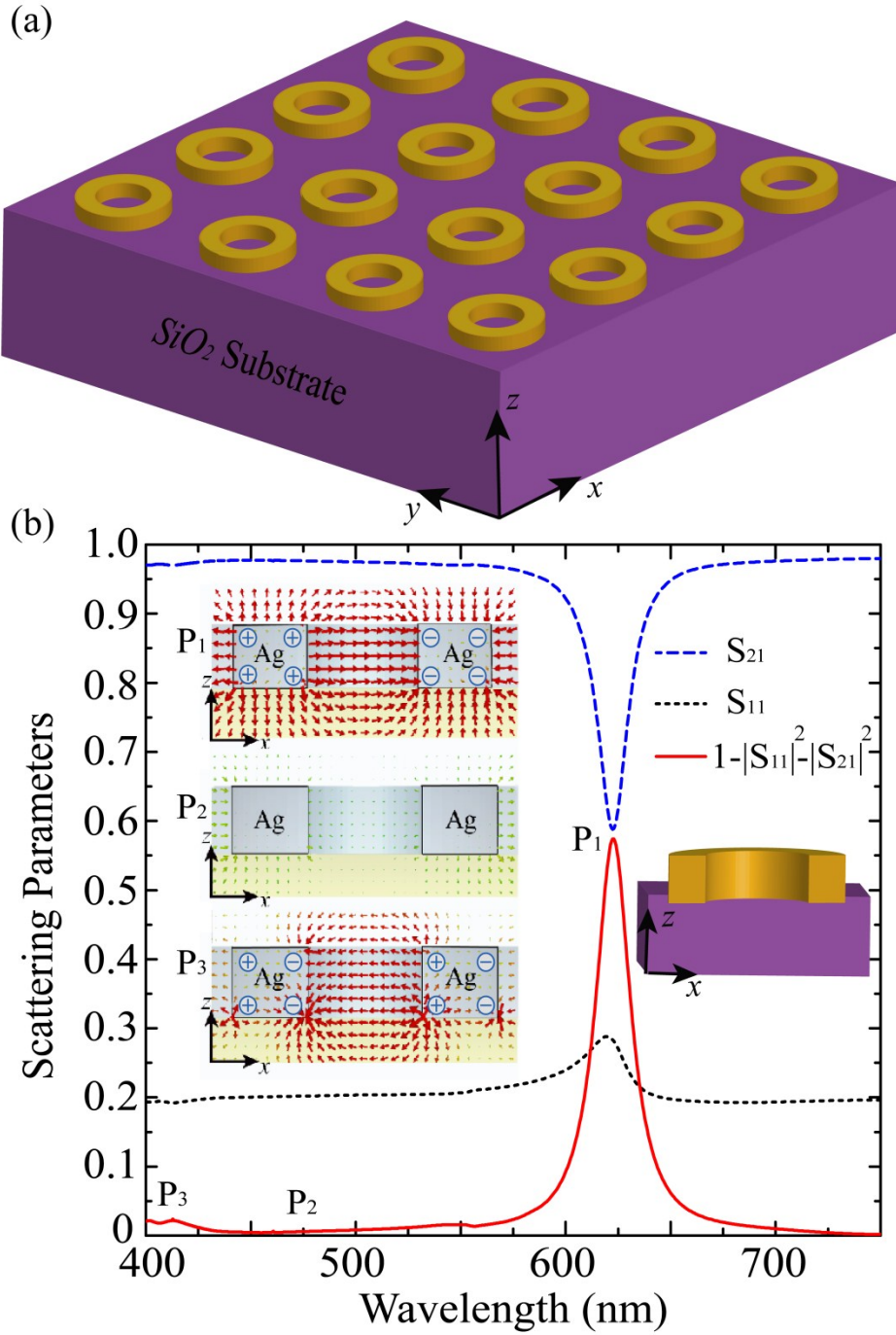


Fig.S2 (a) Schematic of periodically arrayed silver nanorings on the silicon dioxide substrate. (b) The scattering parameters of the structure. The blue dashed curve, the black dot curve and the red solid curve indicate the transmittance, reflectance and absorbance of the structure, respectively. The right inset is the cross section along the x-z plane for the building block. P<sub>1</sub>, P<sub>2</sub>, and P<sub>3</sub> indicate the position where bonding resonance, nonresonance, and weak anti-bonding resonance occur, respectively. The left inset shows the x component fields distribution to cross section along the x-z plane for the silver nanoring, which corresponds to the wavelengths at P<sub>1</sub>, P<sub>2</sub>, and P<sub>3</sub>, respectively. The charges accumulate at the sharp corners of the ring and the red arrows indicate the electric fields.

## 2. The role of numbers of building blocks

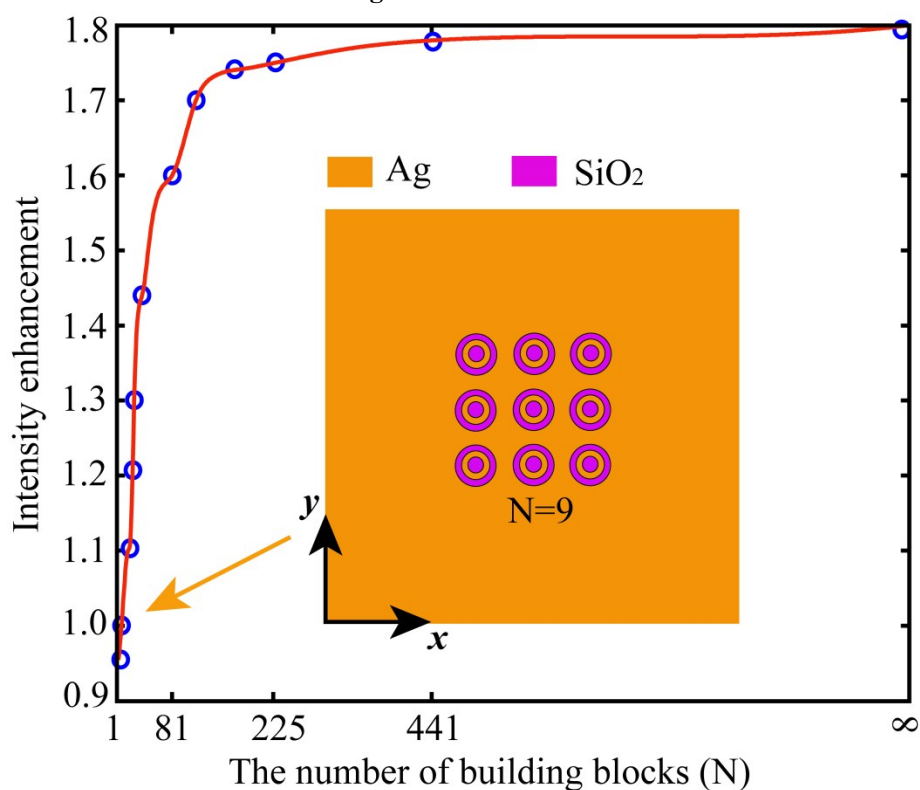


Fig. S3 Intensity enhancement at the focal plane as a function of the number of building blocks. Calculated data are denoted as the blue rings, the red curve represents the fit to the calculated data. The inset shows an example for  $N=9$ . The orange arrow indicates the corresponding intensity enhancement.

The achieved intensity enhancement factor at the focal plane is affected by the finite number of unit cells. In this calculation, the silver film on the substrate is set large enough to avoid the effect of the open boundary. The number of the building blocks in  $x$  direction and  $y$  direction are assured the same and the intensity enhancement is calculated as:  $E_o^2/(E_i^2*2.25)$ , where the  $E_o$  and  $E_i$  denote the field amplitude at the focal plane and the incident light, respectively. The incident environment is  $\text{SiO}_2$  ( $\epsilon=2.25$ ) to simulate the thick enough substrate in reality. Figure S3 shows the dependencies of the intensity enhancement on the total numbers of building blocks  $N$ . The intensity enhancement factor increase rapidly when the  $N$  is lower than 100 and saturate when  $N$  reaches 225, demonstrating that a weak coupling exists between the adjacent unit cells.

## References

- 1 E. Prodan, C. Radloff, N. J. Halas, and P. Nordlander, *Science*, 2003, 302, 419-422.
- 2 P. Nordlander, *ACS Nano*, 2009, 3, 488-492.